Journal of the American Ceramic Society

Predictive, miniature co-extrusion of multi-layered-glass fiber-optic preforms

Journal:	*Journal of the American Ceramic Society*
Manuscript ID:	Draft
Manuscript Type:	Article
Date Submitted by the Author:	n/a
Complete List of Authors:	Bhowmick, Kaustav; National Institute of Technology Sikkim, Electronics and Communication engineering Furniss, David; University of Nottingham, Mechanical, Materials and Manufacturing Engineering Morvan, Herve; University of Nottingham, Mechanical, Materials and Manufacturing Engineering Seddon, Angela; University of Nottingham, Mechanical, Materials and Manufacturing Engineering Benson, Trevor M.; University of Nottingham, Electrical and Electronic Engineering
Keywords:	chalcogenides, extrusion, modeling/model, fibers, optical materials/properties

Predictive, miniature co-extrusion of multi-layered-glass fiber-optic preforms

TITLE

Predictive, miniature co-extrusion of multi-layered-glass fiber-optic preforms

AUTHORS

(1) Kaustav Bhowmick[1]; ph: +919635530509, email: kaustavbhowmickece@gmail.com

(2) David Furniss[2]; email: david.Furniss@nottingham.ac.uk.

(3) Herve P. Morvan[2]; email: herve.morvan@nottingham.ac.uk.

(4) Angela B. Seddon[2]; email: angela.seddon@nottingham.ac.uk

(5) Trevor M. Benson*[2]; ph: +44(0)1159515589, email: trevor.benson@nottingham.ac.uk

[1] Formerly of Faculty of Engineering, University of Nottingham, University Park, Nottingham, Nottinghamshire, NG72RD, UK, now at the Department of Electronics and Communication Engineering, National Institute of Technology, Sikkim, India.

[2]Faculty of Engineering, University of Nottingham, University Park, Nottingham, Nottinghamshire, NG72RD, UK. (* corresponding author)

ABSTRACT

A miniature co-extrusion technique, to produce a concentric multi-layered-glass fiber-optic preform of ~ 3 mm diameter, is modelled and experimentally demonstrated. A three-dimensional, incompressible and non-cavitating, non-isothermal CFD (Computational Fluid Dynamics) model, similar to one developed in our previous work, is used to predict the dimensions of an alternating 4-layer glass-stack feed required to produce the desired layer dimensions in a multi-layered-glass preform extrudate, using a miniaturized and thus more economical co-extrusion. Strong agreement in the cross-sectional geometrical proportions of the simulated and experimentally-obtained preform supports the prowess of the predictive modelling. Nevertheless, some small deviations between the simulated and experimentally obtained dimensions indicate topics for future rheological study. Performing the co-extrusion process under vacuum helps minimize inter-layer defects in the multi-layered fiber-optic preform. The miniature co-extrusion potentially removes the need for a post-extrusion draw-down prior to fiber-drawing, avoiding de-vitrification issues possible in non-oxide novel glass compositions.

Predictive, miniature co-extrusion of multi-layered-glass fiber-optic preforms

Keywords—Co-extrusion, novel glass, fiberoptic preform, CFD.

I. INTRODUCTION

Co-extrusion of polymers [1, 2] and glasses [3] has been undertaken for quite a few decades. As discussed in our earlier work [4], extrusion, as a glass-molding technique, can play an important role in the manufacture of novel glass optical fibers [5-11]. This is because chemical vapor deposition, routinely used to fabricate high silica glass fiber-optic preforms, is usually not appropriate for making non-silica glass fibreoptic preforms due to the disparate vapor pressures of the novel glass constituents and their precursors. The hot ram extrusion technique has been used for forming novel glass fiber-optic preforms. Here we take the example of extrusion of mid-infrared transmitting, chalcogenide glass, fiber-optic preforms. The chalcogenide glasses are atmosphere-sensitive above their glass transition temperature (T_g) [12] and so processing of the glass-supercooled melt under an inert atmosphere, or vacuum, is prerequisite.

It can be observed from [5-11] that hot ram extrusion of novel glasses is usually done on a relatively large-scale. In this previous work, the starting glass-stack feed was generally 18-30 mm in diameter and resulted in a 7-10 mm diameter extrudate. This type of larger-scale extrusion may help off-set any potential for shear-thinning of a glass-melt flowing in contact with the extruder wall; also frictional effects at the static walls during extrusion of a glass melt would tend to be less dominant. The large-scale extruded fiber-optic preforms usually require a post-extrusion cane-drawing, or narrow-down process, prior to the final fiber-drawing. However, each extra forming (*i.e.* shaping) process involves extra heat-treatment of the supercooled glass melt and risks the possibility of, for instance, unwanted devitrification occurring [12, 13] in the

Predictive, miniature co-extrusion of multi-layered-glass fiber-optic preforms

glass fiber-optic preform. Devitrification has the end result of unwanted extrinsic light scattering loss in the finally drawn fiber.

Previous work has shown that core/clad., step-index fiber-optic preform extrudates, made from a bi-layer glass-stack feed, while exhibiting constant outside diameter (OD), displayed a characteristic internal variation along the extrudate-length of the concentric layer thickness (*i.e.* annular ring thickness) of the two glasses making up the rod step-index preform [10, 11]. It is concluded that it is highly desirable to be able to predict and control each individual concentric layer thickness in the resulting extrudate. Our prime target, therefore, has been to demonstrate the ability to model the extrusion process and predict the extrudate geometry resulting from a particular glass-stack feed or *vice versa*. In particular, we wish to predict the extruded preform-length over which the concentric layer dimensions remain uniform, as it is that part of the fiber-optic preform which is best selected for the post-extrusion draw-down, ultimately to make the optical fibre. Modeling the extrusion process to give the ability to design a particular glass-stack feed to produce a particular fiber-optic preform geometry is desirable for attaining the desired optical response in the finally drawn optical fiber.

In our previous work [4], we have developed and validated a Computational Fluid Dynamics (CFD) model which successfully described the geometry of a step-index fiber-optic preform, of nominal outer diameter 9 mm from the larger-scale extrusion of a 30 mm outside-diameter (OD) 2-layer glass-stack feed (the preform had been made earlier [10, 11]).

In contrast, in the present work, using the same CFD framework as described in our earlier work [4], we have been able to *predict* the starting stack arrangement and dimensions required to

produce the specific layer dimensions for a fiber-optic preform designed to have four alternating chalcogenide glass layers and made *via* a *miniaturized* extrusion (see Fig. 1).

The miniaturized system had an extruder barrel of ~ 14 mm internal-diameter (ID) (Fig. 2) and was able to produce fiber-optic preforms with less custom-made glass than in our previous work, using the larger-scale extruder, which had an extruder barrel of 30 mm ID [4]. Applying the miniaturized extrusion to a chalcogenide glass-stack feed, a thin multi-layered extrudate of constant OD, of between about 3 mm and 5 mm, could be directly formed. The miniaturized extrusion of chalcogenide glasses was carried out under vacuum to inhibit oxidation and hydrolysis of the supercooled chalcogenide glass melt. The applied vacuum was expected to help reduce inter-layer defects, such as pores, forming between the mating multi-layer surfaces during the extrusion and in this way to help reduce extrinsic optical scattering loss in the final optical fiber.

As in our previous work [4], simulation and experimental results have been compared, here specifically to make the case for the predictive capability of the modelling approach we are proposing for application to multi-layered extrusion, even with the additional challenge of using miniaturized extruder dimensions.

The same two chalcogenide glass compositions were taken as in our previous work [4], *viz.*: $Ge_{17}As_{18}Se_{65}$ ((atomic% (at%)) which formed here the core and second concentric-ring-layer out from core and $Ge_{17}As_{18}Se_{62}S_3$ (at%), which formed the first and third concentric-ring-layers out from core. Note that the third concentric-ring-layer has been entitled the clad. (d3) in the initial 4-layer glass-stack extrusion feed, in Fig.1(a) and throughout. Also the concentric rings out from the core have been given the nomenclature: d1 and d2 traveling outwards from the core (see

Predictive, miniature co-extrusion of multi-layered-glass fiber-optic preforms

Fig.1(a) and throughout). The viscosity/temperature behavior of $Ge_{17}As_{18}Se_{65}$ is given in [10], together with thermal expansion coefficients and T_g of both glass compositions.

II. MINIATURISED EXTRUDER WITH VACUUM FITTINGS

The essential parts of a glass extruder are a furnace to heat the initial glass-stack feed, to a temperature above the highest glass transition temperature (T_g) of the glasses in the stack to form the supercooled glass-melt phases, and the piston to press these. The stack dimensions drawn in Fig. 1(a) correlate with those of the experimental 4-glass-layer stack feed, shown taken apart in Fig. 7. The extruder undergoing vertical, downwards extrusion is depicted in Figs. 1 (b) and(c) with a schematic of the ensuing cross-section geometry of the extrudate in Fig. 1(d). Finally Fig. 1(e) shows a schematic of the length, L, of the extrudate, whose OD is constant and for which the multi-layer thicknesses inside the extrudate each remain constant along the length L of the extrudate. The significance of L is that this is the key part of the extrudate which is most uniform and hence most suitable to be taken forward for post-extrusion processing, ultimately to draw to fiber of constant and controlled geometry. Note that, although the extrudate OD remained constant over the extrudate length, apart from the very first glass to emerge from the die, the length L of the extrudate (Fig. 1(e)), over which all the internal multi-layer thicknesses remained constant, was a much smaller length of the total extrudate length. L tended to vary with the dimensions of the glass-stack feed and the extrusion process experimental parameters.

As shown in Fig. 2, a free running bobbin was inserted between the piston and the top of the alternating chalcogenide glass 4-layer-stack feed; the bobbin had the purpose of lowering the possibility of adhesion between the piston and the supercooled glass-melt.

Predictive, miniature co-extrusion of multi-layered-glass fiber-optic preforms

The chalcogenide glass 4-layer-stack feed was housed in the extruder barrel and a vacuum imposed. The extrusion die had been internally lined with graphite prior to the extrusion (see Fig 3) in order to reduce the friction imposed on the supercooled glass-melt as it flowed against the die internal wall during the extrusion. The extruder barrel ID (equal to the extrusion die entry ID) was chosen to be 14 mm since the silica glass ampoule containment available to melt directly the chalcogenide glass small-scale boules, required for the extruder-feed layers, were of nominal dimension 13.6 mm / 18 mm = ID / OD, with a view to making ~13.6 mm OD glass cylinders, of circular cross-section, as the extruder feed. A close fit between the extruder barrel ID and the starting glass-stack feed cross-sectional OD was sought in order to minimize the possibility of misalignment of the glass stack whilst loading it into the inside of the extruder barrel, ready for the initial compression of the stack (Fig. 1(c)) [4].

The detailed parts of the miniaturized extruder are given in Fig. 2. From Fig. 2, the miniature stainless-steel extruder barrel was 30 ± 0.25 mm OD and 14 ± 0.25 mm ID. The small notch shown was the point of attachment of the inner barrel to the extruder support and for application of the vacuum environment. The miniature extrusion die had a 14 ± 0.25 mm entry ID and 3.2 mm exit ID (n.b., internally lined with graphite) and the vacuum seal was fitted with heat-resistant rubber O-rings to help maintain the applied vacuum inside the piston / barrel assembly until the multi-layered extrudate was guided out. The arrows in Fig. 2 indicate the direction of fitting of the parts shown with respect to the miniature barrel. Fig. 3 show the graphite-lined small extrusion die in detail, from the side of entry of the glass super-cooled melt to the exit side where the extrudate emerged from the die. As can be seen from Fig. 3, the graphite used was not very fine-grained.

Predictive, miniature co-extrusion of multi-layered-glass fiber-optic preforms

III. CFD PREDICTIVE MODELLING OF MINIATURE 4-LAYER EXTRUSION

The predictive CFD extrusion model we described in [4] was applied here, albeit in a scaled-down geometry from the larger-scale extrusion used in [4]. The internal layer dimensions of the multi-layered fiber-optic preform extrudate were simulated. This approach could be applicable for making a fiber-optic preform to be drawn into large mode area, single mode (LMA-SM) optical fiber [15]. However here, two rather than three glass compositions have been taken to build the initial 4-glass-stack feed, in order to enable exploration of such LMA-SM fiber structures within the compositional range of chalcogenide glasses. This was deemed sufficient to demonstrate the principle and potential of the model for predicting the extrusion process and its outcome.

The target extrudate outer-diameter for the present work was taken as 3.2 mm. Further outer layers of a LMA-SM fiber [15, 16] could be formed in the future by subsequent over-cladding of the four-layer extrudate.

The nomenclature of the numerical domain boundaries of the mesh was set as in [4]. The lengths of the domain wall-boundaries of the mesh used for the present simulation are shown in Table 1 and were obtained by numerical experimentation.

IV. NUMERICAL VERIFICATION OF MESH

The modeling was undertaken using the commercial software ANSYS-CFX [17]. The sensitivity of the predictions to spatial discretization, and in particular to the mesh size, was tested by simulating the extrusion of a four-layer glass-stack with layer-heights of: 10.6 mm (“clad.” in Fig. 1(a)), 7.4 mm, 2.2 mm and 2.2 mm (core) using different mesh sizes, *viz.* with: 176,230

(Mesh 1), 217,635 (Mesh 2), 292,680 (Mesh 3) mesh nodes. The distribution of the mesh nodes was more refined near the curved edge of the die region than at the straight regions of extruder barrel and the outlet (see [4], Fig.1 and Table 1). The meshes used were one volume-element thick [4], since absolute 2-D (2-dimensional) models are not supported in ANSYS-CFX version 13, and the configuration is justified by the cylindrical symmetry of the model and the assumed unidirectional flow observed in glass-extrusion [4]. Using three meshes enables us to measure the rate of change of the solution with change in the mesh size and therefore quantify the sensitivity of the solution to spatial discretization. This is illustrated quantitatively in the next paragraph.

A dynamic-mesh approach was adopted [4] with the ram-movement time-step, $\Delta t = 0.5$ s. A second order advection scheme was used to discretize the convective terms alongside a first-order Euler transient scheme with target convergence criteria for residuals set at 10^{-5} (reduction of the non-dimensional error for each equation by 5 orders of magnitude before marching forward in time to the next timestep) combined with, typically, a maximum of five iterations, per timestep. The four glass volume layers (of the 4-layer glass-stack feed (see Fig. 1(a) and Fig. 4(a)) were represented by a Volume-Of-Fluid (VOF) method as in [4] with a user-defined function, applying a non-isothermal wall-temperature profile obtained approximately from the thermocouple readings obtained from the walls of the actual miniature-extrusion barrel assembly. A sample representation of the model in CFX-POST, the visualization software used by the authors, depicting the glass layers at 1200 secs of the simulation run-time, is shown in Fig. 4(a).

The solutions obtained on each of the three meshes were run successfully to completion of the physical process, *i.e.* until the glass-stack mesh was almost fully extruded) using a timestep $\Delta t = 0.5$ s and compared. Thereafter, the following normalized L2-errors

Predictive, miniature co-extrusion of multi-layered-glass fiber-optic preforms

$$\sqrt{(\Sigma(datd^{i}_{mesh(j-1)} - datd^{i}_{meshj})^2 / \Sigma(datd^{i}_{meshj})^2)},$$

where j = 1, 2, 3, for each of the 3 meshes, and i = time instances from 0 s to completion were calculated between the pairs of meshes 'Mesh1 / Mesh3', 'Mesh1 / Mesh2' and 'Mesh2 / Mesh3', for the emerging glass-melt-extrudate layer-radii for the core and the two successive outer layers out from the core, and the outermost layer thickness in the simulated extrudate, as shown in Fig. 4(b). From Fig. 4(b), it can be seen that the core and the first inner glass layer in the model, which formed the top of the 4-layer glass-stack feed, incurred higher errors than the two lower glass layers. Overall, Mesh3 was deemed suitable as the error between the predictions obtained on two consecutive meshes is below 4% (and generally close to 2.5% between Meshes 2 and 3). After three to five modeling iterations using Mesh3, the stack dimensions required to produce the simulated glass layers close to the intended multi-layer dimensions, in the fiber-optic extrudate, were obtained, as shown in Table 2.

An experiment was then prepared to validate the process using the starting stack dimensions used in the simulation to arrive at the desired extrusion design.

V. EXPERIMENTAL VALIDATION OF SIMULATED RESULTS

For the experimental validation of the simulated results, the starting glass-stack feed dimensions (Fig. 1(a) and Fig. 5), used in the CFD simulation, were used to define the preparation of the experimental glass-stack feed. Note that, at the start of the extrusion process, the 4-glass-stack of 13.6 mm OD underwent an initial 'squashing' under the applied load (schematically shown in Fig. 1(b)), which marked the onset of the extrusion modeling [4].

Predictive, miniature co-extrusion of multi-layered-glass fiber-optic preforms

Chalcogenide glass ($Ge_{17}As_{18}Se_{65}$ and $Ge_{17}As_{18}Se_{65}S_3$ (at %)) rod samples were prepared from precursors as in [4, 11], but in 13.6 mm / 18 mm = ID / OD silica glass ampoules, to fit inside the miniature extruder barrel of ID = 14.0 ± 0.25 mm (see section *II*).

(i) Preparation of glass-stack feed

The as-annealed $Ge_{17}As_{18}Se_{65}$ and $Ge_{17}As_{18}Se_{65}S_3$ (at %) glass rod samples were each sawn (Buehler Isomet diamond wafering saw, oil lubricant, 0.014 mm thick Cu blade) orthogonal to the rod axis, to make two glass cylinders of each composition. The large cross-sectional faces of the sawn four cylinders were each ground (1000 grit Buehler SiC powder) flat and orthogonal to the cylinder axis, to try to match the target height of each cylinder, as presented in Table 2. The actual heights of the cylinders obtained experimentally were then measured with electronic-calipers and are listed in Table 2. A photograph of the prepared glass cylinders is shown in Fig. 5, along with the extrusion die. No further polishing was done of these ground glass cylinders. One $Ge_{17}As_{18}Se_{62}S_3$ glass cylinder had observable cracks on the top surface (see Fig. 5 (b)) but it was still used in the experiment to help observe the effectiveness of the vacuum environment applied, during the extrusion, in reducing inter-layer defects at the mating surfaces of the multi-layers of the extrudate.

In the simulated stack, the ratio of the heights of the glass cylinders from the outer-most layer in the extrudate to core, was: 4.82 : 3.36 : 1 : 1 (Table 2). The ratio in the actually obtained glass cylinder set was rather: 5.03 : 3.68 : 0.95 : 1, as shown in Fig.5 (a)-(e) and Table 2. Hence, there were unintended dimensional errors incurred during the experimental preparation of the 4-layer glass-stack comprising the 4 prepared cylinders. Therefore when extruding fiber-optic preforms, it is helpful to understand the physical tolerance of the optical fiber performance to its geometry.

Predictive, miniature co-extrusion of multi-layered-glass fiber-optic preforms

As can be seen in [15, 16] the optical response may be tolerant to changes in the layer dimensions in LMA-SM fiber designs.

(ii) Co-extrusion of 4-layer extrudate

The four chalcogenide glass cylinders (prepared as in section *V(i).*) were stacked vertically, to form the 4-layer glass-stack feed, inside the miniature extruder barrel, and were placed above the die and under the punch in the extruder (Fig. 1). Glass cylinder 1 was placed at the top of the stack (extrudate core) and glass cylinder 4 (named d3 'clad.' in Fig. 1(a)) was placed at the bottom of the stack. The overall co-extrusion procedure followed the schematic procedure in Fig. 1. The bobbin was placed gently on top of the 4-layer glass-stack and the extrusion furnace was raised so that the barrel assembly was sitting within the hot zone of the furnace. Next, the extruder was closed off to the external atmosphere at the extreme bottom. The hydraulic ram was then lowered from above into the furnace and left about 2 mm above the topmost glass layer to allow for a stress-free thermal expansion of the glasses, and of the supercooled glass-melts, during the initial heating up of the extruder assembly. The lowering of the ram resulted in the top of the assembly becoming closed off to the external atmosphere, as a heat-resistant O-ring vacuum-seal located itself at the neck of the barrel. The vacuum pump was turned on and was left to pump down to ≤ 10 Pa. Then the furnace was turned on and the temperature was raised from ambient up to 280°C (*ca.* [T_g + 50°C] of the glass compositions). The system was left to equilibrate thermally. At 280°C, the ram was moved to make contact with the top of the stack *via* the bobbin. The mechanically elastic glasses had been heated and, above T_g, had transformed to supercooled liquids which exhibited viscous flow. Thus the glass melts slumped down to fill the gap between the outside of the circular-cross-section stack and the inside of the larger circular

cross-section of the miniature extruder barrel, which had had the 2 mm clearance on first loading the 4-layer glass-stack feed into the extruder at ambient temperature.

Next, controlled movement of the hydraulic piston was applied and the load (nominal 61.5 kg) was put into operation and the furnace set temperature was raised to 290°C. The temperature and load were gradually, manually, increased until a nominal constant-velocity movement of the piston, bobbin and glass-melt in unison was reached and sustained under a load of 321.5 kg at an observed die temperature of 316°C, for a set furnace temperature of 310°C.

The applied load, temperature and displacement of the bobbin were recorded using Picolog software (www.picotech.com). The average velocity of the top bobbin was ~ 0.11 mm min^{-1} for steady extrusion of the $Ge_{17}As_{18}Se_{65}$ / $Ge_{17}As_{18}Se_{62}S_3$ multi-layered preform. At temperatures > 310°C the effects of viscous flow of the supercooled glass-melts were observed as forming (shaping) of the preform extrudate occurred and it started to emerge from the die. The extrusion took 45 min to complete. Note that the initial heating up and thermal equilibration of the extruder equipment prior to the extrusion took several hours.

At the end of the extrusion, the local vacuum was slowly replaced by nitrogen (oxygen free, black-flagged, 'BOC', UK) introduced into the extruder at 8.3 m^3/s. Then the furnace was switched off and allowed to cool down slowly to room-temperature with the extrudate left in place within the thermal mass of the extruder, thereby effecting annealing of the extrudate.

It is interesting to note that the set furnace temperature of 310°C here was close to the 305°C temperature at the die observed during the large-scale extrusion previously conducted by Savage *et al.* [10, 11], using the same glass pair as here: $Ge_{17}As_{18}Se_{65}$ / $Ge_{17}As_{18}Se_{62}S_3$ but in a bi-glass-stack for co-extrusion to form a core / clad. step-index fiber-optic preform, which was then

drawn to step-index fiber. Savage *et al.* [10, 11] reported that the extrusion took place steadily at a supercooled glass-melt viscosity of $10^{7.75}$ Pa.s whereas here a die temperature of 316°C implies extrusion at $< 10^{7.5}$ Pa.s

VI. RESULTS OF EXTRUSION

The small-scale extrusion under vacuum of the 4-glass-stack resulted in an extrudate comprising and internal geometry of (see Fig. 1): core, $Ge_{17}As_{18}Se_{65}$; 1st layer out from core (d1) $Ge_{17}As_{18}Se_{62}S_3$; 2nd layer out from core (d2), $Ge_{17}As_{18}Se_{65}$ and clad. (d3), $Ge_{17}As_{18}Se_{62}S_3$. The rod extrudate was axially straight and 350 mm long (*i.e.* 350 mm from the die-end (the last glass to emerge from the die) to the rounded end (the first glass to exit the die, datum D), and had an OD of 3.19 mm ± 0.014 mm over the 350 mm length (see section *VI(ii)* for measurement details). The extrudate was glossy in appearance and without any visible surface defects, as shown in Fig. 6(a). However, some glass had been lost to the process due to overflowing of the supercooled melt during the extrusion across the top of the die and the bobbin, as shown in Figs. 6(b) and (c).

(i) Preparation of samples for extrudate characterization

The 350 mm long extruded preform was carefully sectioned orthogonal to the preform rod axis (Buehler Isomet saw; 0.014 mm thick copper blade) into 17 cylindrical pieces, each nominally of equal axial length, named: P1 to P17. For pieces P3 to P17 (for which the simulation suggested there should be internal geometry due to multi-layering), each circular face was ground flat with 1000 grit Buehler SiC powder and then polished to a 3 μm finish with diamond paste (Buehler).

Predictive, miniature co-extrusion of multi-layered-glass fiber-optic preforms

One notch-arrow was mechanically scored in the glass outer surface at approximately the center of each cylindrical piece P3-P17 (see Fig. 6d). This directional notching was done because it was known that the visible contrast between the glass pair $Ge_{17}As_{18}Se_{65}$ and $Ge_{17}As_{18}Se_{62}S_3$ was neither distinct to the naked eye nor under the optical microscope [10, 11]. On the other hand, good imaging contrast was found under scanning electron microscopy (SEM), due to the chemical-compositional contrast of the two glasses caused by the presence/absence of sulfur. Retention of the one notch-arrow at the center of the side of each piece enabled measurement of the true distance of each cross-sectional circular face of each sawn piece from the start of the preform, datum 'D'. This was important because there was unintentional material loss during the grinding and polishing operations necessary in order to render the surface quality good enough to capture the SEM images for measurement of the required dimensions.

(ii) Sample characterization

The OD of each piece P1 to P17 was measured using electronic Vernier calipers, taking the average of 5 readings for each piece. Next each of the two cross-sectional circular faces, of each cylindrical piece P3 to P17, was carbon coated and then subjected to back-scattered electron (BSE) and secondary electron (SE) SEM-imaging under an XL-30 FEG-ESEM (field emission gun, environmental SEM). The diameter and thickness of each of the four glass concentric layers within each cylindrical piece P3 to P17, comprising the extruded rod preform, were noted at the interfaces; the dimensional variation of these along the axial length of the fiber-optic rod preform was collated.

Fig. 7 shows typical ESEM- SE and ESEM-BSE images to allow comparison of the surface views and features; the lighter and the darker layers correspond to the Ge-As-Se and Ge-As-Se-S

compositions, respectively. The black spots seen on the sample surface in Fig. 7 appear to be debris. ESEM-EDX analysis gave the observed glass compositions (error expected: ± 0.5 at%) as: $Ge_{17.24}As_{17.35}Se_{65.23}$ (expected $Ge_{17}As_{18}Se_{65}$) and $Ge_{16.95}As_{17.76}Se_{62.04}S_{3.22}$ (expected $Ge_{17}As_{18}Se_{62}S_3$), respectively, lying within the expected error.

VII. COMPARISON OF EXPERIMENTAL AND SIMULATED RESULTS

A modified, final CFD simulation was run using the actual experimental 4-layer glass-stack dimensions (to account for human-errors in preparing the glass slabs), along with the observed die temperature, used at boundary condition for the wall during the miniature extrusion (see section *V(ii)*). Mesh3 was used for this final calculation.

The experimental layer dimensions within the sectioned multi-layer preform extrudate, taken from the ESEM imaging, were collated. These were taken as the layer radius relative to the extrudate radius of the core and next two layers, out from the core, and the outer layer thickness of the third layer from the core (termed clad. in Fig. 1(a)); about 9 measurements for each layer radius (core, d1, d2) and thickness (d3, 'clad.') were obtained from each ESEM image of each side of each cylindrical sectioned piece P3 to P17.

The experimental glass-layer dimensions thus obtained were plotted as a function of linear position from the start of the extrudate (*i.e.* from the datum point D, Fig. 6(a), (d) and Fig 8) along with the respective layer dimensions predicted by the CFD model. This point is shown in Fig. 8.

Predictive, miniature co-extrusion of multi-layered-glass fiber-optic preforms

VIII. DISCUSSION

(i) Physical quality of the experimentally obtained miniature extrudate fiber-optic preform

All the inter-layer defects observed within the extruded multi-layer extrudate were found to be associated with the $Ge_{17}As_{18}Se_{62}S_3$ / $Ge_{17}As_{18}Se_{65}$ glass layer boundary of d2 (2^{nd} layer out from the core) with the d3 clad., shown in Fig. 7. This originated from the glass cylinder d2 which had exhibited residual cracks in the top surface prior to being stacked inside the extruder barrel (see Fig. 5b). Nevertheless, the use of the vacuum for extrusion seems to have been beneficial in reducing the severity of the effects.

The step-index fiber-optic preform extrudate reported by Savage *et al.* [10-11] was extruded under an atmosphere of flowing argon; the preform exhibited some pores along the bi-layer interface, specifically traceable to that length of the interface where the two faces of the bi-layer glass stack had first mated during the extrusion process, accompanied by, presumably, entrenchment of the local gas atmosphere. The present extrudate was mostly free of such defects.

Also, in the current work, the glass layers in the extrudate were at times rather uneven in their thickness and some squashing of the inner layers by the outer layers rendering a more obvious off-roundedness [10-11] in the inner-layers near to the core. This resulted in a larger variation of the plots in Fig.8 of the inner-layer dimensions than found for the outer layer dimensions. Hence some distortions in the inner layer shapes of the extrudate appear to have developed within the supercooled glass-melt flow. This might be alleviated in the future by extruding at a greater viscosity, closer to 10^8 Pa.s, (*cf.* here < $10^{7.5}$ Pa.s, whereas ~ 10^8 Pa.s is used in [3-11]). On the other hand, the outermost layer dimensions might have suffered from variations due to the supercooled glass-melt flowing over the coarse grade of graphite lining the die. In order to

control this, finer grade graphite might be used in the die in the future in an attempt to lower the friction between the flowing supercooled glass-melt and the die internal wall. This would enable the use of a lower temperature and load for the extrusion which would in turn reduce the speed of flow of glass-super-cooled-melt through the die.

(ii) Comparison of experimental and simulated results

For the multi-layered glass-stack miniature extrusion, close agreement was found with the glass layer dimensions from the CFD simulation model, without any numerical modification over [4], can be seen in Fig. 8(a-d).

The predicted core-radius was the most greatly varying layer along the axial length of the extruded preform, at about 10% above the experimental value, as it became closer to the end of the preform. However, the optical fiber designs, prepared from such extrudates, usually have a larger dimensional tolerance (e.g. at least 20%) [15, 16] for the desired optical performances. Further, the scaling of glass-layer sizes, when drawing the intended fiber from the extrudate, is mostly linear [11]. As stated above (section *VIII(i)*), the miniature extrusion was carried out at an observed die temperature of 316^{o}C, and a glass-melt viscosity closer to 10^{7} Pa.s, than the 10^{8} Pa.s more often employed in the larger-scale extrusions [3-11].

Overall, the comparison between the experimental results and the simulated results, as shown in Fig.8, further supports the claim made by the authors in relation to the predictive capability of the proposed CFD-based tool [4] and enables an approximate tracking of the glass layers formed during extrusion, within a good tolerance, for the subsequent identification of the best extrudate region for fiber drawing. However, if a more definite prediction of the layer dimensions is needed, detailed rheological studies on flow of chalcogenide supercooled glass-melts in intimate

contact with each other will need to be done in the future, for molding purposes and for cost-effective use of expensive glass.

IX. CONCLUSIONS

We have demonstrated a miniature extrusion technique for making chalcogenide glass fiber-optic preforms. By experimentally demonstrating the miniature extrusion of a 4-layer LMA-SM type fiber-optic preform, the usefulness of the process has been flagged for multi-layered multi-glass preforms. A vacuum environment was applied as opposed to nitrogen / inert gas in established methods, which has been effective in reducing interfacial defects in the extruded preform (especially, compared to previous extrusion work under a gaseous atmosphere, of entrenched bubbles at the first mating interface), despite one glass cylinder having sustained severe surface damage prior to the extrusion. In previous work we have presented a CFD model, of the extrusion process, which showed promise for working as a predictive tool for preparing core/clad., and step-index fiber-optic preforms and fiber [4, 10, 11]. In the present work the same model, albeit with scaled down dimensions according to the miniaturized extrusion undertaken, was used to predict the dimensions of the starting chalcogenide glass-stack needed to produce a given preform with four glass regions of required dimensions. The model successfully showed its capability as a tool for predicting the layer dimensions in the actual extrudate. Using this predictive tool one might confidently identify the linear and useful zone in an extrudate without a *post-mortem* 'chopping up' of the preform which is a destructive type of analysis. Such a predictive approach is also cost effective, as it limits the number of experiments needed. The slight deviations of the experimental results from the simulated results may be attributed to: (a)

the use of a coarse quality graphite as the die-lining and/or, (b) the unknown rheological properties of chalcogenide glasses in the supercooled phase state of glass-melt-on-glass-melt flow, absent in the model, and which warrants future experimental study, as well as (c) remnant numerical errors from the discretization and iterative processes, and, of course, modeling errors.

Predictive, miniature co-extrusion of multi-layered-glass fiber-optic preforms

REFERENCES

[1] M. Mignanelli, K. Wani, J. Ballato, S. Foulger and P. Brown, '*Polymer microstructured fibers by one-step extrusion*', Opt. Express, 15[10], 6183-6189, (2007).

[2] M. Ferenets, H. Myllymaki, K. Grahn, A. Sipila and A. Harlin, '*Manufacturing methods for multi step index plastic optical fiber materials*', AUTEX Research Journal, 4[4], 164-174, 2004.

[3] D. Furniss and A. B. Seddon, '*Extrusion of gallium lanthanum sulphide glasses for fiber-optic preforms*,' J. Mat. Sci.Letts. 17, 1541-1542, (1998)

[4] K.Bhowmick, H.P. Morvan, D. Furniss, A.B. Seddon and T.M. Benson, '*Co-extrusion of multi-layer glass fiber-optic preform: prediction of layer dimensions in the extrudate*', Journal of the American Ceramic Society, 96[1], 118-124, (2012).

[5] H. Ebendorff-Heidepriem and T. M. Monro, '*Analysis of glass flow during extrusion of optical fiber preforms*', Opt. Mat. Express, 2[3], 304-320 (2012).

[6] A. B. Seddon ; D. Furniss and A. Motesharei, '*Extrusion method for making fiber optic preforms of special glasses*.,' Proc. SPIE 3416, Infrared Glass Optical Fibers and Their Applications, 32 (1998); doi:10.1117/12.323398.

[7] H. Ebendorff-Heidepriem and T. M. Monro, '*Extrusion of complex preforms for microstructured optical fibers*,' Optics Express, 15, 15086-15092 (2007).

Predictive, miniature co-extrusion of multi-layered-glass fiber-optic preforms

[8] X. A. Feng, T. M. Monro, P. Petropoulos, V. Finazzi and D. J. Richardson, '*Extruded single-mode high-index-core one-dimensional microstructured optical fiber with high index-contrast for highly nonlinear optical devices*,' Applied Physics Letters, 87, 081110 (Aug 22, 2005), DOI:http://dx.doi.org/10.1063/1.2034094

[9] D. J. Gibson and J. A. Harrington, '*Extrusion of hollow waveguide preforms with a one-dimensional photonic bandgap structure*, ' Journal of Applied Physics, 95[8], 3895-3900 (2004).

[10] S. D. Savage, C. Miller, D. Furniss, and A. B. Seddon, '*Extrusion of chalcogenide glass preforms and drawing to multimode optical fibers*,' J. Non-Cryst. Solids, 354, 3418–27 (2008).

[11] S.D. Savage, 'Development of low optical loss chalcogenide fibers for mid-infrared transmission', PhD thesis, Faculty of Engineering, University of Nottingham, (Nov. 2005).

[12] A. B. Seddon, '*Chalcogenide glasses - a review of their preparation, properties and applications*,' J Non-Cryst Solids, 184, 44-50 (1995)

[13] H. Rawson, *Glass Science and Technology, Properties and Applications of Glass*. (Elsevier Scientific, 1980).

[14] H. L. Rowe, 'Infra-red transmitting optical fibres with potential use in medical diagnosis and treatment,' PhD thesis, Faculty of Engineering, University of Nottingham, (2008).

[15] K. Bhowmick, 'Coextrusion of multi-layered multi-glass fiber-optic preforms for infrared applications,' PhD thesis, Faculty of Engineering, University of Nottingham, UK (2013).

[16] A. Kumar, V. Rastogi, C. Kakkar and B. Dussardier, '*Co-axial dual core resonant leaky fiber for optical amplifiers*,' J. Opt. A: Pure Appl. Opt. 10 115306 (2008) doi:10.1088/1464-4258/10/11/115306

[17] *ANSYS CFX, "Release 13, User Manual," http://www.ansys.com/corporate/locations.asp (accessed 12 September, 2012)*

Predictive, miniature co-extrusion of multi-layered-glass fiber-optic preforms

LIST OF FIGURES

Fig.1. Schematic of the fiber-optic preform extrusion process. (a) Initial feed glass-feed comprising an alternating 4-layer glass stack; the dimensions shown tally with the experimental glass feed (taken apart) in Fig. 7. (b) Initial squashing of the supercooled glass-melt layers under the applied load, to fill the extrusion barrel chamber. Note that the die exit internal diameter: δ = 3.2 mm. (c) Process of extrusion under the applied load. (d) Schematic end-on of extrudate cross-section. (e) Extrudate indicating the region "L" over which the dimensions of the multi-layers, which comprised the extrudate, remained constant; the extrudate outside diameter was constant. (b)-(d) adapted from [14]

Fig. 2. Parts of the small-scale extrusion assembly fabricated in-house: (a) bobbin which was positioned on top of the glass-stack feed and beneath the piston; (b) stainless steel, small-scale extruder barrel of 30 ± 0.25 mm OD and 14±0.25 mm ID; (c) small extrusion die of 14 ± 0.25 mm entry ID and 3.2mm exit ID; the die was internally lined with graphite and (d) the vacuum seal fixture fitted with a heat-resistant O-ring. The horizontal arrows show the direction of fit of each part into the others.

Fig. 3. The graphite-lined stainless-steel extrusion die used during the miniature extrusion shown in detail: (a) the top of the extrusion die where the starting multi-layer glass-stack rested before the vertical, downward extrusion was begun and (b) the lower end of the extrusion die through which the supercooled glass-melt extrudate exited the die downwards during the extrusion process.

Fig.4. CFD set up and numerical verification for layer measurements: (a) quasi-isometric view of planes 1 and 2, as in [4], for data representation at 1200 s (the x,y, and z show the orientation of the Cartesian coordinate system along which the model is aligned, i.e., extrusion happens in +x-direction); (b) L2-error % estimation between pairs of Meshes for the glass-layer radii for the core and the two successive outer layers, d1, d2, respectively, from the core and for the glass-layer thickness for the outermost Ge-As-Se-S layer (d3) (see Fig. 1(a)) in the simulated extrudate, viz. Mesh1-Mesh3, Mesh1-Mesh2 and Mesh2-Mesh3.

Fig.5. The prepared chalcogenide glass cylinders for the miniature extrusion: (a) $Ge_{17}As_{18}Se_{62}S_3$ (atomic %) glass cylinder: 9.96 mm high (for 'clad' layer: d3 [15, 16]); (b) $Ge_{17}As_{18}Se_{65}$ glass cylinder 7.29 mm high (for 2nd layer out from core: d2 [15, 16]); (c) $Ge_{17}As_{18}Se_{62}S_3$ glass

cylinder 1.88 mm high (for 1st layer out from core: d1 [15, 16]); (d) $Ge_{17}As_{18}Se_{65}$ glass cylinder 1.98 mm high (for core) and (e) graphite lined extrusion die. The damage at the top of glass cylinder: d2 shown in (b) was deliberately left in place to test the ability of the miniature extrusion process, carried out under vacuum, to heal the damage at this surface as this surface mated with the under surface of glass cylinder d1 (c) during the extrusion process.

Fig.6. (a) The 350 mm long fiber-optic preform extrudate from the miniature extrusion done under vacuum; the start of the preform is marked as the datum 'D'. (b) Glass layer left on top of extrusion die of thickness (< 0.5 mm). (c) Glass from original 4-layer glass-stack feed now sticking on to the bobbin after the extrusion. (d) Chopping schema for the extruded preform starting from the datum, D, to the end, E, with each piece marked at center (except for the first one), numbered from P1 to P17, as shown. The two sides of each piece can be designated as PnD and PnE (n = 1 to 17), designating whether the end is closer to datum D or to end E, respectively.

Fig.7. ESEM images of cylindrical pieces P11-E (please see nomenclature in Fig.7(d)) and P12-E (see Fig. 7(d)): (a) ESEM-BSE image P11-E under 15 kV accelerating voltage and minimum magnification showing the glass layers formed (core, d1 (1st layer out from core), d2 (2nd layer out from core), d3 ('clad.'), designated as in figure 1(a); (b) ESEM-SE image of P11-E showing the absence of any inter-layer defects; (c) ESEM-BSE image of P12-E showing the layers and one possible inter-layer defect encircled, and (d) ESEM-BSE image of P12-E (light grey layers - $Ge_{17}As_{18}Se_{65}$, dark grey layers - $Ge_{17}As_{18}Se_{62}S_3$). The regions enclosed in red lines were designated as possible inter-layer defects under ESEM-BSE, but later confirmed as debris using ESEM-BSE.

Fig.8. Measured layer radii, or layer thickness, of the extruded $Ge_{17}As_{18}Se_{65}$ / $Ge_{17}As_{18}Se_{62}S_3$ four-layer preform, plotted against distance from the start of the extrudate (datum D, Fig.7(a) and (d)), compared to respective layer radii from CFD simulation of the miniature extrusion: (a) core radius; (b d1, 1st layer out from core = $Ge_{17}As_{18}Se_{62}S_3$ layer radius; (c) d2, 2nd layer out from core: $Ge_{17}As_{18}Se_{65}$; (d) clad. $Ge_{17}As_{18}Se_{62}S_3$ thickness. (Error bars are of the order: 10^{-2}-10^{-3} mm.)

Predictive, miniature co-extrusion of multi-layered-glass fiber-optic preforms

LIST OF TABLES

TABLE I. Typical Extrusion model wall-boundaries and relevant lengths in the model after the initial slump-down of the original 4-layer glass-stack which marked the start of the simulation.

TABLE II Glass cylinder dimensions in the 4-layer glass-stack feed used in the initial simulation feed; glass cylinder dimensions in the 4-layer glass-stack feed made experimentally and then used in the modified final simulation.

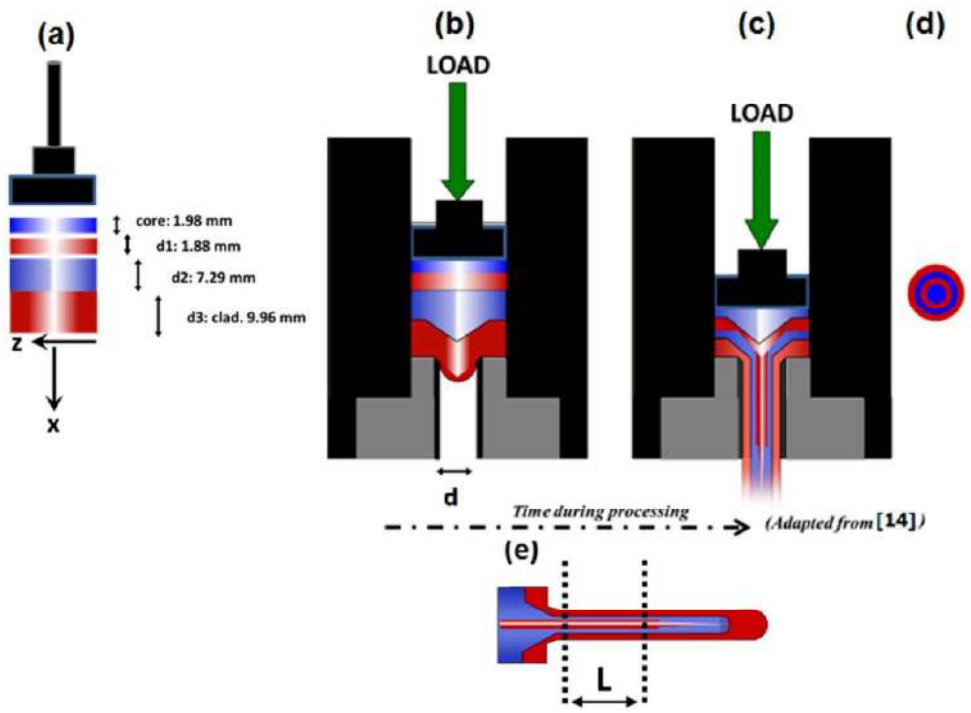

Fig. 1 Schematic of the fiber-optic preform extrusion process. (a) Initial feed glass-feed comprising an alternating 4-layer glass stack; the dimensions shown tally with the experimental glass feed (taken apart) in Fig. 7. (b) Initial squashing of the supercooled glass-melt layers under the applied load, to fill the extrusion barrel chamber. Note that the die exit internal diameter: δ = 3.2 mm. (c) Process of extrusion under the applied load. (d) Schematic end-on of extrudate cross-section. (e) Extrudate indicating the region "L" over which the dimensions of the multi-layers, which comprised the extrudate, remained constant; the extrudate outside diameter was constant. (b)-(d) adapted from [14]
84x59mm (300 x 300 DPI)

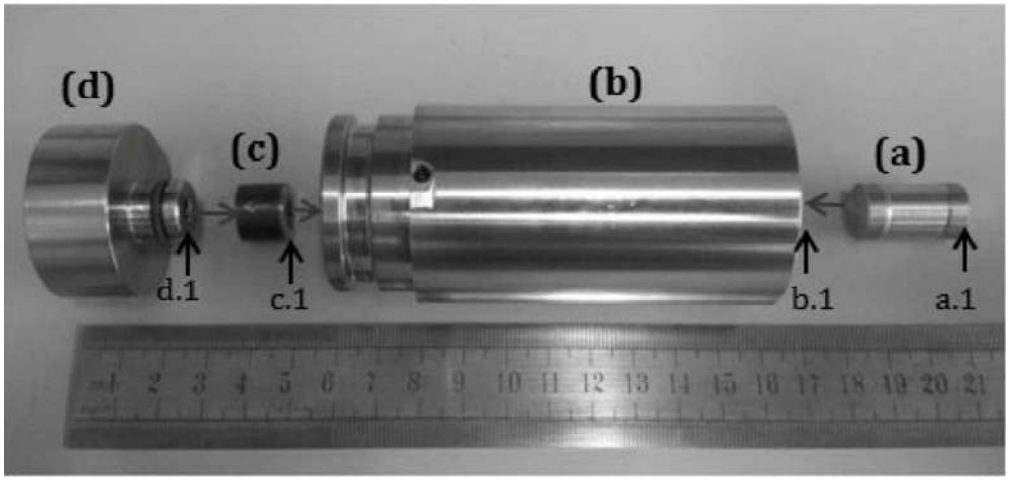

Fig. 2 Parts of the small-scale extrusion assembly fabricated in-house: (a) bobbin which was positioned on top of the glass-stack feed and beneath the piston; (b) stainless steel, small-scale extruder barrel of 30 ± 0.25 mm OD and 14±0.25 mm ID; (c) small extrusion die of 14 ± 0.25 mm entry ID and 3.2mm exit ID; the die was internally lined with graphite and (d) the vacuum seal fixture fitted with a heat-resistant O-ring. The horizontal arrows show the direction of fit of each part into the others.
84x40mm (300 x 300 DPI)

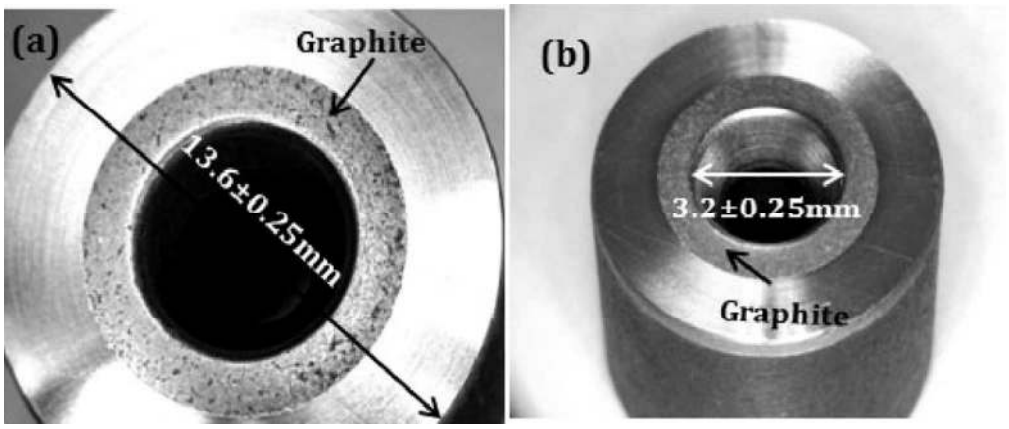

Fig. 3 The graphite-lined stainless-steel extrusion die used during the miniature extrusion shown in detail: (a) the top of the extrusion die where the starting multi-layer glass-stack rested before the vertical, downward extrusion was begun and (b) the lower end of the extrusion die through which the supercooled glass-melt extrudate exited the die downwards during the extrusion process.
84x35mm (300 x 300 DPI)

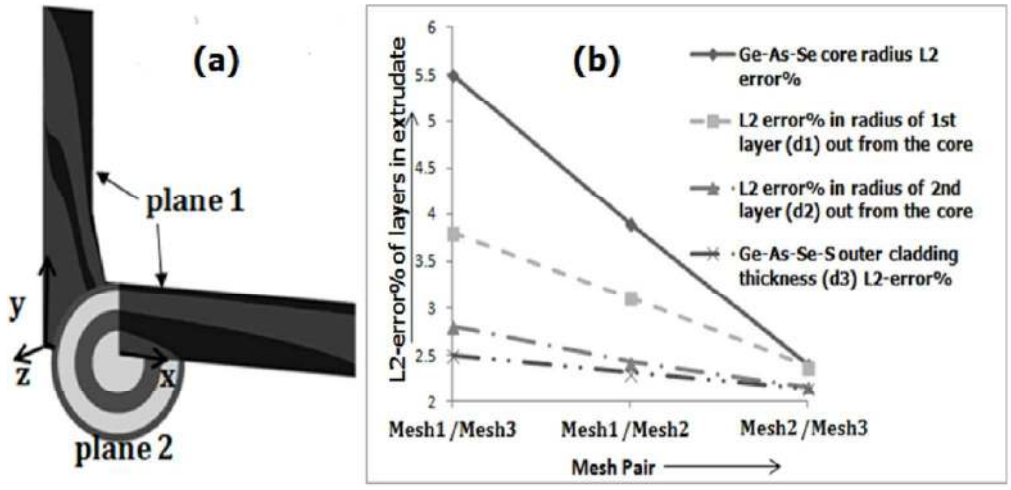

Fig. 4 CFD set up and numerical verification for layer measurements: (a) quasi-isometric view of planes 1 and 2, as in [4], for data representation at 1200 s (the x,y, and z show the orientation of the Cartesian coordinate system along which the model is aligned, i.e., extrusion happens in +x-direction); (b) L2-error % estimation between pairs of Meshes for the glass-layer radii for the core and the two successive outer layers, d1, d2, respectively, from the core and for the glass-layer thickness for the outermost Ge-As-Se-S layer (d3) (see Fig. 1(a)) in the simulated extrudate, viz. Mesh1-Mesh3, Mesh1-Mesh2 and Mesh2-Mesh3. 84x40mm (300 x 300 DPI)

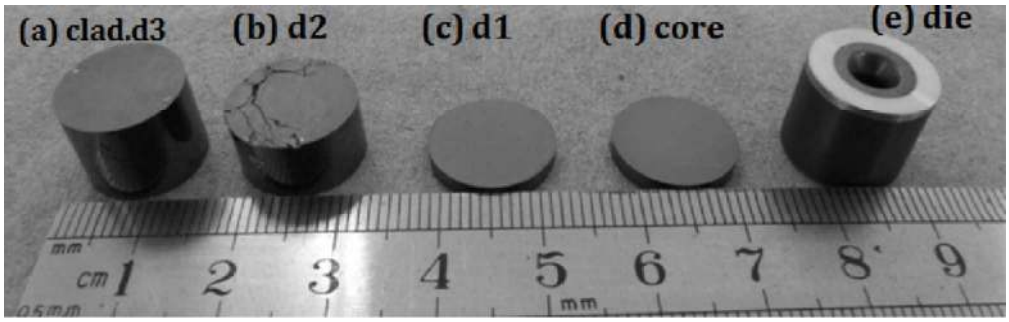

Fig. 5 The prepared chalcogenide glass cylinders for the miniature extrusion: (a) Ge17As18Se62S3 (atomic %) glass cylinder: 9.96 mm high (for 'clad' layer: d3 [15, 16]); (b) Ge17As18Se65 glass cylinder 7.29 mm high (for 2nd layer out from core: d2 [15, 16]); (c) Ge17As18Se62S3 glass cylinder 1.88 mm high (for 1st layer out from core: d1 [15, 16]); (d) Ge17As18Se65 glass cylinder 1.98 mm high (for core) and (e) graphite lined extrusion die. The damage at the top of glass cylinder: d2 shown in (b) was deliberately left in place to test the ability of the miniature extrusion process, carried out under vacuum, to heal the damage at this surface as this surface mated with the under surface of glass cylinder d1 (c) during the extrusion process.
84x26mm (300 x 300 DPI)

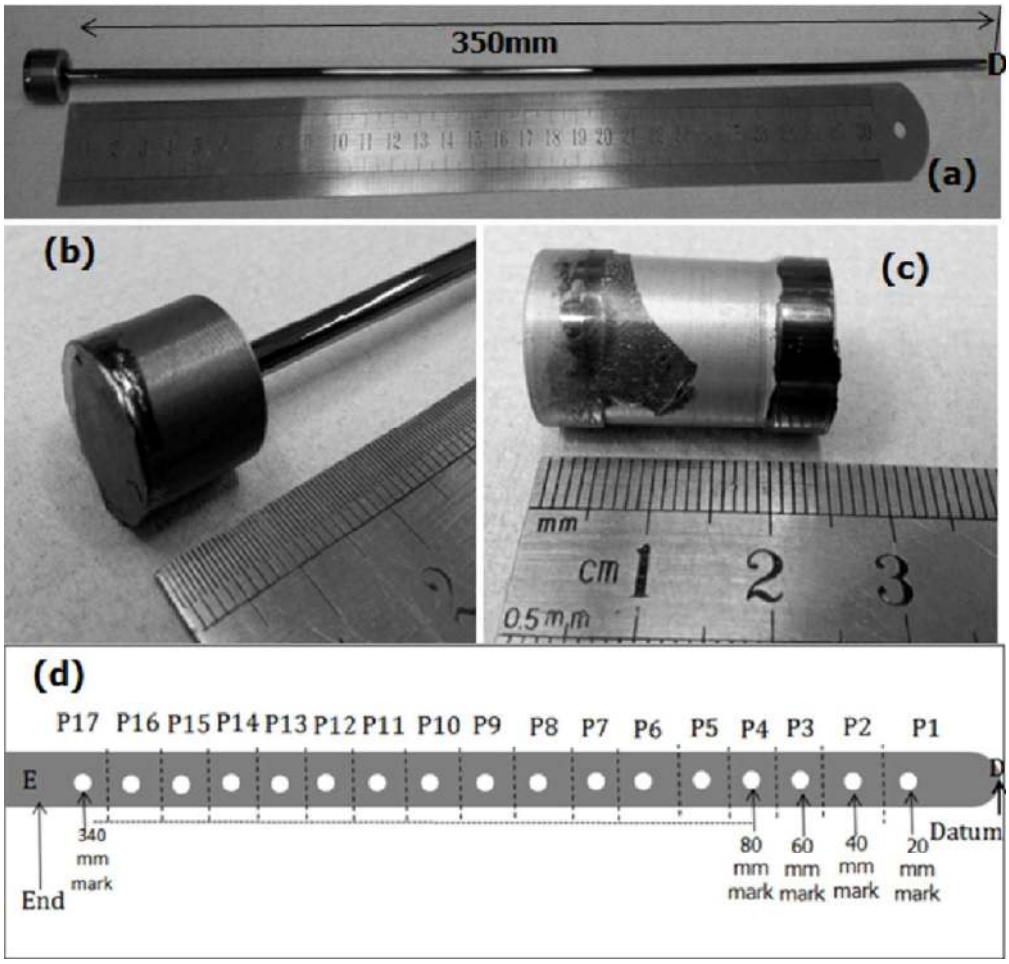

Fig. 6 (a) The 350 mm long fiber-optic preform extrudate from the miniature extrusion done under vacuum; the start of the preform is marked as the datum 'D'. (b) Glass layer left on top of extrusion die of thickness (< 0.5 mm). (c) Glass from original 4-layer glass-stack feed now sticking on to the bobbin after the extrusion. (d) Chopping schema for the extruded preform starting from the datum, D, to the end, E, with each piece marked at center (except for the first one), numbered from P1 to P17, as shown. The two sides of each piece can be designated as PnD and PnE (n = 1 to 17), designating whether the end is closer to datum D or to end E, respectively.
68x65mm (300 x 300 DPI)

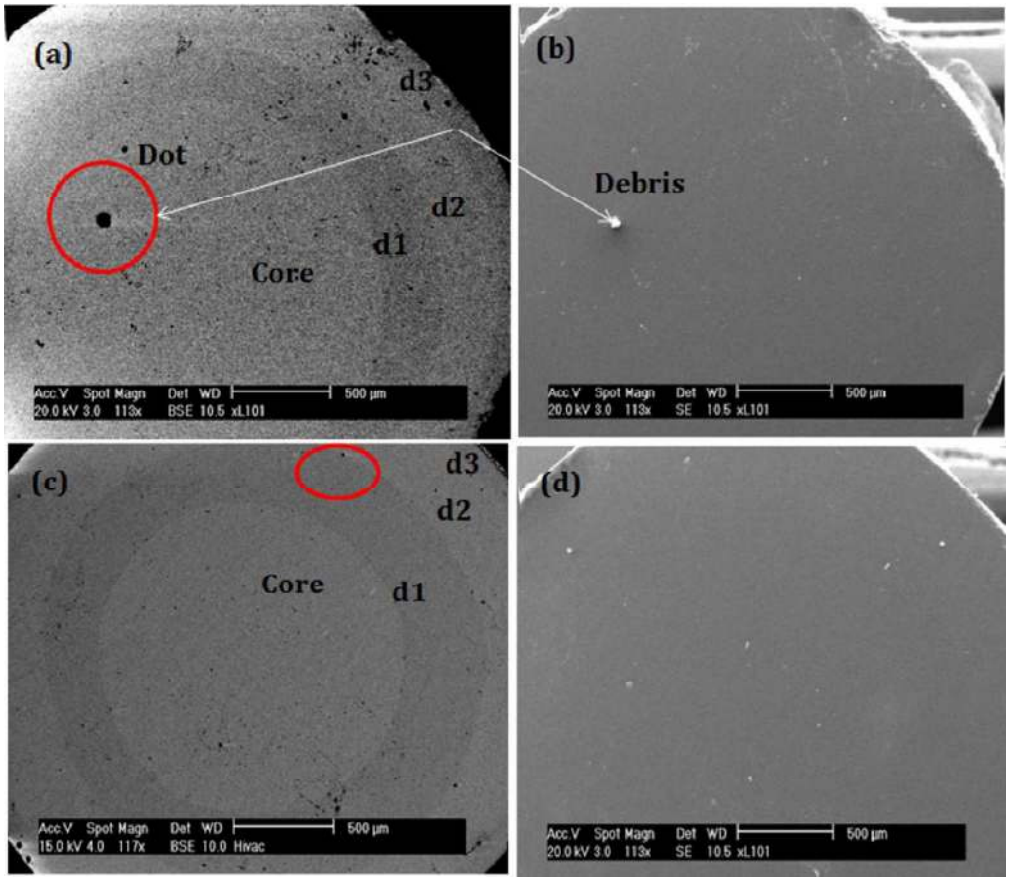

Fig. 7 ESEM images of cylindrical pieces P11-E (please see nomenclature in Fig.7(d)) and P12-E (see Fig. 7(d)): (a) ESEM-BSE image P11-E under 15 kV accelerating voltage and minimum magnification showing the glass layers formed (core, d1 (1st layer out from core), d2 (2nd layer out from core), d3 ('clad.'), designated as in figure 1(a); (b) ESEM-SE image of P11-E showing the absence of any inter-layer defects; (c) ESEM-BSE image of P12-E showing the layers and one possible inter-layer defect encircled, and (d) ESEM-BSE image of P12-E (light grey layers - $Ge_{17}As_{18}Se_{65}$, dark grey layers - $Ge_{17}As_{18}Se_{62}S_3$). The regions enclosed in red lines were designated as possible inter-layer defects under ESEM-BSE, but later confirmed as debris using ESEM-BSE.
74x65mm (300 x 300 DPI)

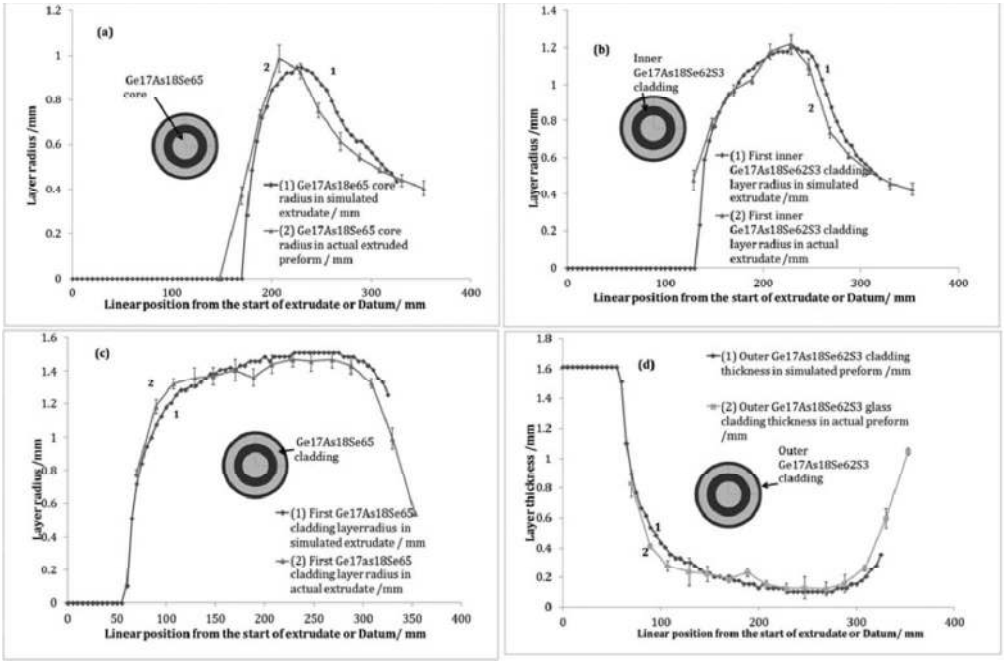

Fig. 8 Measured layer radii, or layer thickness, of the extruded Ge17As18Se65 / Ge17As18Se62S3 four-layer preform, plotted against distance from the start of the extrudate (datum D, Fig.7(a) and (d)), compared to respective layer radii from CFD simulation of the miniature extrusion: (a) core radius; (b d1, 1st layer out from core = Ge17As18Se62S3 layer radius; (c) d2, 2nd layer out from core: Ge17As18Se65; (d) clad. Ge17As18Se62S3 thickness. (Error bars are of the order: 10-2-10-3 mm.)
84x55mm (300 x 300 DPI)

Model boundaries [4].	Boundary location [4]	Length / mm
p	Extruding piston (top)	7.0
u	Inner walls of upper extruder barrel	22.4
b1	Top flat surface and slanted inlet wall of the die with internal graphite lining.	6.87
b2	Straight lower section of die supporting glass flow	6.19
L	Lower domain wall initially filled with air	410
O	Outlet of model	1.6

Glass composition	Position of glass-layer starting from the top of the glass-stack feed as placed inside the extruder barrel.	Target glass cylinder thickness from initial simulation / mm.	Observed glass cylinder thickness after laboratory preparation; also these dimensions were used for the modified, final simulation / mm.
$Ge_{17}As_{18}Se_{65}$	1 (core.)	2.20	1.98
$Ge_{17}As_{18}Se_{62}S_3$	2	2.20	1.88
$Ge_{17}As_{18}Se_{65}$	3	7.40	7.29
$Ge_{17}As_{18}Se_{62}S_3$	4 (clad.)	10.60	9.96